



Original article

Discovery of novel selective inhibitors of *Staphylococcus aureus* β -ketoacyl acyl carrier protein synthase III

Jee-Young Lee, Ki-Woong Jeong, Soyoung Shin, Ju-Un Lee, Yangmee Kim*

Department of Bioscience and Biotechnology, Bio/Molecular Informatics Center, Konkuk University, 1 Hwayang-dong, Gwangjin-gu, Seoul 143-701, South Korea

ARTICLE INFO

Article history:

Received 29 June 2011

Received in revised form

22 October 2011

Accepted 28 October 2011

Available online 4 November 2011

Keywords:

KAS

Fatty acid synthesis

Antibiotics

In silico screening

MRSA

ABSTRACT

β -Ketoacyl-acyl carrier protein synthase III (KAS III) is a condensing enzyme in bacterial fatty acid synthesis and a potential target while designing novel antibiotics. In our previous report, we discovered the lead compound YKAs3003, which serves as an inhibitor of *Escherichia coli* KAS III (ecKAS III), and determined a reliable pharmacophore map from *in silico* screening. In this study, we determined two pharmacophore maps from receptor-oriented pharmacophore-based *in silico* screening of the x-ray structure of *Staphylococcus aureus* KAS III (saKAS III) to identify potent saKAS III inhibitors. We discovered a new potential inhibitor (**6**) with broad-spectrum antimicrobial activity and 0.8 nM binding affinity for saKAS III, proving the reliability of our pharmacophore map. Using optimization procedures, we identified three new antimicrobial saKAS III inhibitors: **6c** (2,4-dichloro-benzoic acid (2,3,4-trihydroxy-benzylidene)-hydrazide), **6e** (4-[(3-chloro-pyrazin-2-yl)-hydrazonomethyl]-benzene-1,3-diol), and **6** (4-[(5-trifluoromethyl-pyridin-2-yl)-hydrazonomethyl]-benzene-1,3-diol). All three inhibitors have a novel 4-hydrazonomethyl-benzene-1,3-diol core structure. These inhibitors exhibited high binding affinity to saKAS III and highly selective antimicrobial activities against *S. aureus* and methicillin-resistant *S. aureus*, with minimal inhibitory concentration values of 1–2 μ g/mL.

© 2011 Elsevier Masson SAS. All rights reserved.

1. Introduction

During the past 60 years, antimicrobials have been defending against infectious diseases caused by several bacteria, virus and other pathogenic microorganisms. However, many target microorganisms have become resistant to antimicrobials; this is an increasing public health problem [1]. MRSA is the most common resistant microbe that is primarily associated with healthcare-related infection; infection and antibiotic resistance of MRSA are increasing worldwide [2,3]. The severity of the antimicrobial drug resistance of MRSA requires the development of new antibiotics against it and other pathogens. To overcome this resistance problem, the identification of antimicrobial compounds that have a novel mechanism of action towards new target enzymes, such as those involved in bacterial fatty acid biosynthesis, is critical [4,5].

Fatty acids are a main source of energy in bacterial cells and they play an important role in the formation of cell membranes [6,7].

The microbial fatty acid biosynthetic pathway contains several potential therapeutic targets for antimicrobial and antimalarial drugs [7]. Fatty acid synthase (FAS), a multifunctional enzyme complex system, regulates fatty acid biosynthesis. As shown in Fig. 1, the biosynthetic process is initiated by a condensing enzyme, β -ketoacyl-acyl carrier protein synthase III (KAS III), which is encoded by the *FabH* gene [8,9].

KAS III exists as a homodimers, and contains a catalytic triad formed by the three residues Cys–His–Asn in the active site. These residues are highly conserved in the KAS III of various bacteria [10]. KAS III is an initiation enzyme in fatty acid synthesis, and plays an essential role in bacterial fatty acid biosynthesis [11]. Because the 3D structure of KAS III and its functions are highly conserved in various bacteria, its inhibitors are powerful antibiotics with broad-spectrum activities against gram-negative and gram-positive bacteria [8].

The 3D structures of KAS III and co-complex structures with their inhibitors have been identified in various bacteria by means of x-ray crystallography. The first x-ray structure of KAS III was identified in *Escherichia coli* (*E. coli*) by Rock et al. by using a coenzyme A (CoA) substrate [12]. The structure of *Staphylococcus aureus* (*S. aureus*) KAS III (saKAS III) was identified by Khandekar et al., and that of *Enterococcus faecalis* (*E. faecalis*) KAS III (efKAS III) was determined by Appelt et al. [13,14]. KAS III inhibitors have been

Abbreviations: KAS III, β -Ketoacyl acyl carrier protein synthase III; ecKAS III, *E. coli* KAS III; saKAS III, *S. aureus* KAS III; efKAS III, *E. faecalis* KAS III; HBD, hydrogen bonding donor; HBA, hydrogen bonding acceptor; Lipo, lipophilicity; LigScore, ligand score.

* Corresponding author. Tel.: +82 2 450 3421; fax: +82 2 447 5987.

E-mail address: ymkim@konkuk.ac.kr (Y. Kim).

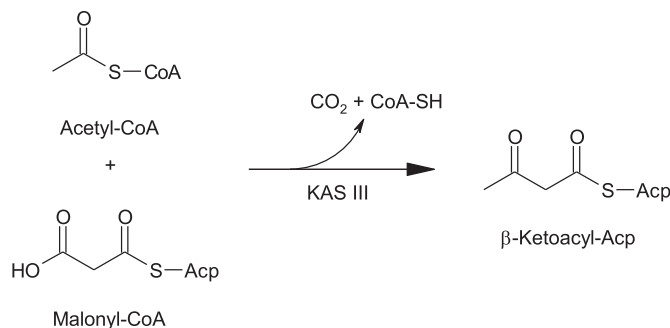


Fig. 1. KAS III initiates the condensation step in FAS II.

designed by using diverse methods. For example, Head et al. determined the first x-ray co-crystal structure of *E. coli* KAS III (ecKAS III) and a small inhibitor, and successfully designed a dichlorobenzyloxy-indole-carboxylic acid inhibitor of KAS III [15]. Thiolactomycin (TLM) and celurenin are the only known antibiotics that inhibit KAS III [9,16]. Many researchers have synthesized derivatives of these two antibiotics to develop potent antimicrobial inhibitors of KAS III. Townsend et al. and Dowd et al. have designed derivatives of TLM as inhibitors of the type I FAS system [17,18]. TLM-independent inhibitors have also been developed. Chu et al. discovered novel potent KAS III inhibitors by using an automated docking procedure [19]. Reynolds et al. designed disulfide KAS III inhibitors against methicillin-resistant *S. aureus* (MRSA) and *Bacillus anthracis* [4] and reported that sulfonyl-naphthalene-1,4-diols act as KAS III inhibitors [20]. The Schiff base, which has the structure of an azomethine moiety ($-C=N-$), is an important functional group in medicine [21]. The Schiff ligand shows antimicrobial activity against various bacteria, including inhibitors of KAS III. Zhu et al. used a Schiff base-containing thiazole or salicylaldehyde template as a substructure for the antimicrobial inhibitors of KAS III [22,23]. Cho et al. and Kaskhedikar et al. performed quantitative structure-activity relationships (QSAR) to design KAS III inhibitors [24–26].

In our previous study, we performed a receptor-oriented pharmacophore-based *in silico* screening of ecKAS III and identified a synthetic lead compound, YKAs3003, with weak antimicrobial activity [27]. A second *in silico* screening for natural compounds identified two flavonoids, YKAF01 (phloretin) and YKAF04 (3,6-dihydroxyflavone), as inhibitors of ecKAS III with strong antimicrobial activity [28]. These two procedures established the accuracy and specificity of our pharmacophore map (Map I). Map I is composed of three features (Fig. 2A): two hydrogen bond donors (HBD1 and HBD2) and one hydrophobic interaction (Lipo1).

In this study, we performed a receptor-oriented pharmacophore-based *in silico* screening of saKAS III by using two maps to find potent saKAS III inhibitors. We identified and optimized novel potent KAS III inhibitors that displayed powerful antimicrobial activities against *S. aureus* and MRSA, with strong binding affinity to saKAS III.

2. Materials and methods

2.1. Building of compound databases

We built a compound database including about 750,000 compounds which collected from ChemBridge Corporation (San Diego, CA) and Specs.net (Kluyverweg, Netherlands). Also, an analogue database was built, including 430 analogues of **6**. The 430 analogues which include 4-iminomethyl-benzene-1,3-diol

or 4-hydrazonomethyl-benzene-1,3-diol, were selected from a 750,000-compound library. All compounds were converted to 3D databases with multiple conformers by applying the catDB utility program, as implemented in DS modeling (Accelrys, Inc., San Diego, CA). We built a 3D compound database with multiple conformers based on the default parameters [29,30]. The parameters are detailed in our previous report [27].

2.2. Receptor-oriented pharmacophore-based *in silico* screening of saKAS III

We defined the active site of saKAS III, based on the center and radius of the binding substrate in an x-ray structure of ecKAS III complexed with CoA. Interaction models were generated within 10 Å of the active site center, and the features adjusted taking into account the substrate binding model. Among the multiple pharmacophore maps, the most favorable binding model of protein and substrate was established via test *in silico* screening with CoA. Pharmacophore maps that effectively expressed the binding model of enzyme with substrate were selected for searching the compound library.

Using selected pharmacophore maps, we searched the compound database. Candidate compounds are selected by chemical property estimations (LigScore, ALogP, and PSA) [27]. All computational procedures were performed on a Linux environment using the DS modeling/SBP module (Accelrys, Inc.) [31].

2.3. Expression and purification of saKAS III

saKASIII were expressed in *E. coli* BL21 (DE3) and purified. The pET-15b/KAS III plasmid was transformed into the expression host. All expression and purification procedures were performed as described previously [27,32]. The gene encoding saKAS III was obtained by PCR with a set of primers (5'-gttcaactatgaacgtgggt-3' and 5'-tgttgttttgacatcattaccga-3') and subcloned into *Bam*HI–*Eco*RI sites of the pGEX-4T-1 expression vector (GE Healthcare), resulting in pGEX-saKAS III coding for a glutathione S-transferase (GST)–saKAS III fusion protein. The recombinant saKAS III was expressed in *E. coli* (DE3) as a GST fusion protein and purified from the supernatant of disrupted cells by GSTrap column (Amersham Pharmacia Biotech). To remove the GST moiety, the fusion protein was incubated with 1:10 (mg/unit) thrombin in PBS buffer (10 mM Na₂HPO₄, 2 mM KH₂PO₄, 137 mM NaCl, 2.7 mM KCl, pH 7.4) for 12 h at room temperature. Once digestion is complete, GST was removed by a GSTrap column. At each stage of the purification process, SDS-PAGE was applied to identify the saKAS III-containing fraction.

2.4. Fluorescence quenching analysis

We added saKAS III protein (10 μM) to buffer (50 mM sodium phosphate, 100 mM NaCl, pH 8.0) and titrated each candidate inhibitor to a final protein-to-inhibitor ratio of 1:10. All solutions contained similar buffer concentrations. The sample was placed in a 2 mL thermostatted cuvette, with excitation and emission path lengths of 10 nm. Using tryptophan emission, we determined the fluorescence quantum yields of KAS III and the ligand. The detailed methods are provided in a previous article [27].

2.5. Antimicrobial activity

We examined the antimicrobial activities of the inhibitor candidates using the standard 2-fold serial broth dilution method [33] with 1 g-negative bacterium (*E. coli* [KCTC 1682]) and 4 g-positive bacteria (*S. aureus* [KCTC 1621], *E. faecalis* [KCTC 2011], MRSA [CCARM 3114], and VREF [clinically isolated]). *E. coli* [KCTC

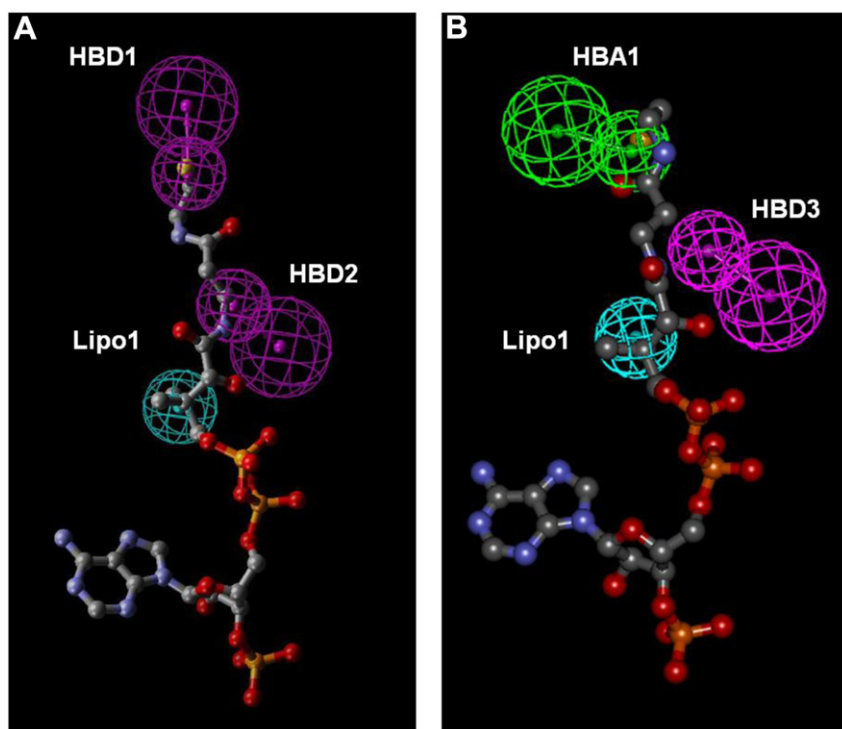


Fig. 2. Results of our two receptor-oriented pharmacophore-based *in silico* screening. (A) Pharmacophore map I (Map I) used for discovery of initial antimicrobial inhibitors. (B) Pharmacophore map II (Map II).

1682] was purchased from the Korean Collection for Type Cultures, Korea Research Institute of Bioscience & Biotechnology (Taejeon, Korea). *E. faecalis* [KCTC 2011], MRSA [CCARM 3114], and VREF [clinically isolated]) were supplied from the Culture Collection of Antibiotic-Resistant Microbes (CCARM) at Seoul Women's University in Korea [34]. The bacterial suspension was adjusted to 0.5 McFarland standard prepared from a single colony on an agar plate incubated for 18–24 h and diluted 10-fold in Mueller Hinton broth. A 20 μ L aliquot of the diluted cell suspension (1×10^6 colony forming units) was used to inoculate each well of a 96-well plate containing 100 μ L of the same medium with the indicated concentrations of candidate inhibitors. The plates were incubated at 37 $^{\circ}$ C for 20 h. We defined minimal inhibitory concentration (MIC) as the lowest concentration of antibiotic leading to complete inhibition of visible growth in relation to an antibiotic-free control well. Experiments were replicated at least 3 times to verify methodology reproducibility using the above conditions.

2.6. MTT assay for cytotoxicity

Mouse fibroblast NIH-3T3 cells were obtained from the Korea Research Institute of Chemical Technology (KRICT, Daejeon, Korea). Cells were cultured in RPMI 1640 supplemented with 10% FBS and antibiotic–antimycotic solution (100 units/mL penicillin, 100 g/mL streptomycin, and 25 g amphotericin B) in 5% CO_2 at 37 $^{\circ}$ C. Cultures were passed every 3–5 days, and cells were detached by a brief trypsin treatment and visualized with an inverted microscope. Cells were maintained in suspension or as monolayer cultures and subcultured. Cytotoxicity against mammalian cells of the compounds was evaluated using an MTT assay. The cells were seeded to each well of a plate containing 100 μ L of cell suspension (2×10^4 cells/well) and then incubated at 37 $^{\circ}$ C in a 5% CO_2 atmosphere for 24 h. Various concentrations of compounds were added to the plate, which was then incubated for an additional 24 h.

After the 24-h incubation, 20 μ L MTT solution was added to each well, and the plate was incubated for another 4 h. The amount of resulting formazan was determined by measuring the absorbance at a wavelength of 570 nm using a microplate reader [35–37]. Using phase contrast microscopy (Motic AE31 with a Moticam 2300), we photographed the cells to determine their morphology after the 24-h culture.

3. Results and discussion

3.1. Receptor-oriented pharmacophore-based *In Silico* screening of saKAS III

Since the co-complex structure of substrate and saKAS III has not been determined, we adapted the binding interactions of substrate-saKAS III based on the x-ray co-complex structures of eckKAS III and efKAS III. We performed *in silico* screening on each x-ray structure: model 1 is a modified binding model of CoA and eckKAS III (1HNJ.pdb) [38], and model 2 is based on the CoA-efKAS III (3IL4.pdb) and inhibitor-efKAS III (3IL5.pdb) co-complexes [13].

In model 1, pharmacophore maps were generated from the interaction and exclusion models by all possible combinations of the three chemical features. Nine pharmacophore maps were generated, and only one (Map I) effectively represented the binding model of substrate-KAS III in each model. Map I is composed of three pharmacophore features: two hydrogen bond donors (HBD1 and HBD2), which are related to the backbone oxygen atoms of Gly203 and Phe298, respectively, and one hydrophobic interaction (Lipo1) with Leu156, Phe157, and Met201. This map corresponds to the map determined from eckKAS III in our previous reports [27,28].

In the x-ray structure of CoA-efKAS III, the carboxyl oxygen of CoA formed hydrogen bonds with the side chains of Asn280 and His250 in Cys-His-Asn catalytic triad, which corresponds to Asn268 and His238 in saKAS III, respectively [13]. In the x-ray structure of

inhibitor-efKAS III, the inhibitor formed these hydrogen bonds with the side chains of Asn280 and His250. Furthermore, there was an additional hydrogen bonding interaction with the backbone nitrogen of Phe224, corresponding to Phe207 in saKAS III. On the basis of this binding information, we determined a second pharmacophore map (Map II) as shown in Fig. 2B. Map II consists of three chemical features: HBA1, HBD3, and Lipo1. HBA1 represents hydrogen bonding with Asn268 and His238, while HBD3 involves hydrogen bonding with the backbone of Phe207. Lipo 1 is identical in Map I and Map II.

Based on Map I and II, we performed an *in silico* screening procedure and searched a compound database composed of 750,000 synthetic compounds. About 2700 compounds were hit by the two maps; we initially selected 100 potential KAS III inhibitor candidates based on estimation of the highest ranked ligand scores (LigScore) [39,40]. Our two previous *in silico* screening procedures confirmed the reliability of Map I and successfully determined the specification of inhibitors through two chemical properties: AlogP and polar surface area (PSA) [41,42]. These chemical properties are related to the binding affinity and the cell permeability of KAS III inhibitors. AlogP values in the range of 2–3.5 and PSA values in the range of 55–100 Å² increase the probability of a compound being a potent inhibitor of KAS III. We selected ten final candidate compounds that satisfied one of these two criteria. The chemical structures of these candidates are shown in Fig. 3. Seven compounds (1–7) were hit by Map I, and three (8–10) were hit by Map II.

3.2. Binding assay using fluorescence quenching

The dissociation constant (K_d) of nine candidates and a reference molecule, TLM, which is a known KAS III inhibitor, were determined by fluorescence quenching experiments with saKAS III [43]. The dissociation constant (K_d) of compounds are listed in Table 1. Three of the candidate compounds (2, 5, and 9), as well as TLM, bind saKAS III with 2–3-digit micromolar binding affinities. 8 and 10 had a micromolar dissociation constant for saKAS III. 6 binds tightly to

Table 1

Chemical properties (PSA and AlogP), MIC against various bacteria, and dissociation constants (K_d) of ten candidate saKAS III inhibitors.

Compound	PSA	AlogP	MIC (μg/mL)					K_d (μM)
			<i>E. coli</i>	<i>E. faecalis</i>	VREF	<i>S. aureus</i>	MRSA	
TLM	62.6	2.62	128	256	128	256	128	55.4
YKAs3003	52.82	3.12	128	256	nd ^a	256	128	nd
1	40.5	2.46	>512	>512	>512	>512	>512	>1000
2	90.6	1.86	>512	256	>512	>512	256	44.0
3	99.4	0.32	>512	>512	>512	>512	>512	>1000
4	98.7	0.83	256	256	32	256	256	>1000
5	79.9	0.46	>512	>512	>512	>512	>512	34.1
6	77.7	3.30	512	64	32	2	4	0.0008
7	100.6	1.55	>512	>512	>512	>512	>512	>1000
8	98.7	2.42	>512	>512	256	>512	>512	0.36
9	110.29	2.84	>512	128	256	>512	>512	649
10	108.99	2.88	>512	256	256	>512	>512	3.18

nd^a is not detected.

KAS III with a nanomolar (0.8 nM) dissociation constant. Fluorescence titration curves of 6 binding to saKAS III are shown in Fig. 4.

The chemical properties of the four compounds (1, 3, 4, and 7) that did not bind to saKAS III are shown in Table 1. 1 has a PSA value under 50, while 3, 4, and 7 have AlogP values less than 2. Therefore, PSA and AlogP values were correlated with binding affinity. Based on these results, we proposed that the six strongly binding compounds (2, 5, 6, 8, 9, and 10) could be potential inhibitors of saKAS III.

3.3. Antimicrobial activities of candidate compounds

We measured the minimal inhibitory concentration (MIC) values of the ten candidate compounds against a gram-negative bacterium (*E. coli*), 2 g-positive bacteria (*S. aureus* and *E. faecalis*), and two resistant bacteria (MRSA and vancomycin-resistant *E. faecalis* (VREF)) (Table 1). Only one compound, 6, displayed broad-spectrum antimicrobial activity against all gram-positive and resistant bacterial strains in the range of 2–64 μg/mL 6

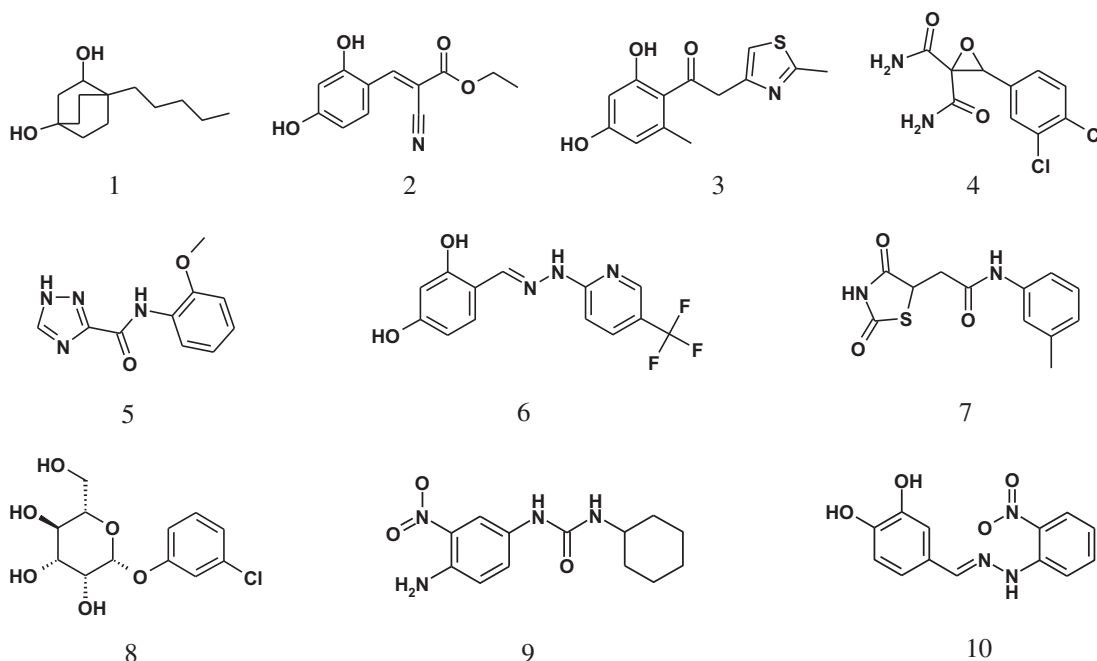


Fig. 3. The chemical structures of the ten candidate saKAS III inhibitors obtained from *in silico* screening for saKAS III.

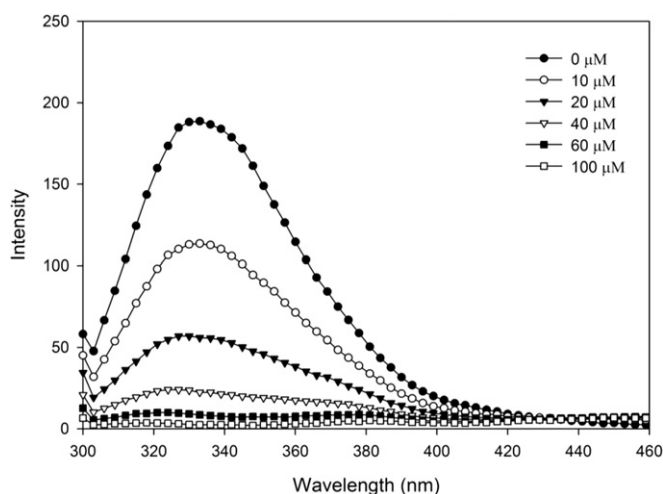


Fig. 4. Fluorescence spectra of saKAS III in the presence of **6**.

showed very strong activity against *S. aureus* and MRSA, especially at 2–4 $\mu\text{g/mL}$. It showed much more potent antibacterial activity compared with TLM: the MIC of TLM was in the range of 128–256 $\mu\text{g/mL}$ [28]. These results agree with those obtained from the binding assay described in the previous section.

Even though compound **2** and **5** bind tightly to saKAS III, they did not have any antimicrobial activity, implying that they might have difficulties in penetrating the bacterial cell membrane. AlogP values were analyzed for these two compounds: **2** and **5** have AlogP lower than 2 (0.46 and 1.86), which are lower than the other candidate compounds. Therefore, we reconfirmed the correlation between the two chemical properties (PSA and AlogP) and the biological activities of the antimicrobial inhibitors of KAS III, as suggested in our previous article.

Compound **8**, **9** and **10**, which were hit by Map II, satisfied the PSA and AlogP criteria and showed good binding affinity for saKAS III. Unfortunately, they showed very low antimicrobial activity against VREF and they did not display antimicrobial activity against *S. aureus* and MRSA. Map II was determined based on the binding model of a substrate or inhibitor to efKAS III and involves hydrogen bonding with Asn268, His238, and Phe207. From our experimental results, these interactions are characteristic of saKAS III binding, but they may not be critical for antimicrobial activity against *S. aureus* and MRSA. Future work will involve revising Map II to develop a more selective antimicrobial inhibitor of saKAS III.

3.4. Binding model of **6** and saKAS III

Compound **6** (4-[(5-trifluoromethyl-pyridin-2-yl)-hydrazono-methyl]-benzene-1,3-diol) contains a benzene-1,3-diol moiety: two hydroxyl oxygen atoms of the diol participate in the hydrogen-bonding interactions with the backbone carbonyl oxygen atoms of Gly203 and Phe298. The pyridine ring of **6** forms a hydrophobic interaction with Thr153, Leu156, and Met201 of saKAS III. The trifluoromethyl group of **6** forms a new hydrophobic interaction with Trp32 and Thr37 at the end of the binding site. This additional interaction, which was not included in our previous study of inhibitors of efKAS III, may enhance the binding affinity, resulting in the increased antimicrobial activity of this compound. The proposed interaction model of **6** and saKAS III is shown in Fig. 5A.

Interestingly, YKAs3003, which was discovered as an efKAS III inhibitor in our previous study, and **6** both have a benzene-1,3-diol moiety, which forms hydrogen bonds with KAS III that contribute to the binding affinity of the KAS III inhibitors. On the other hand,

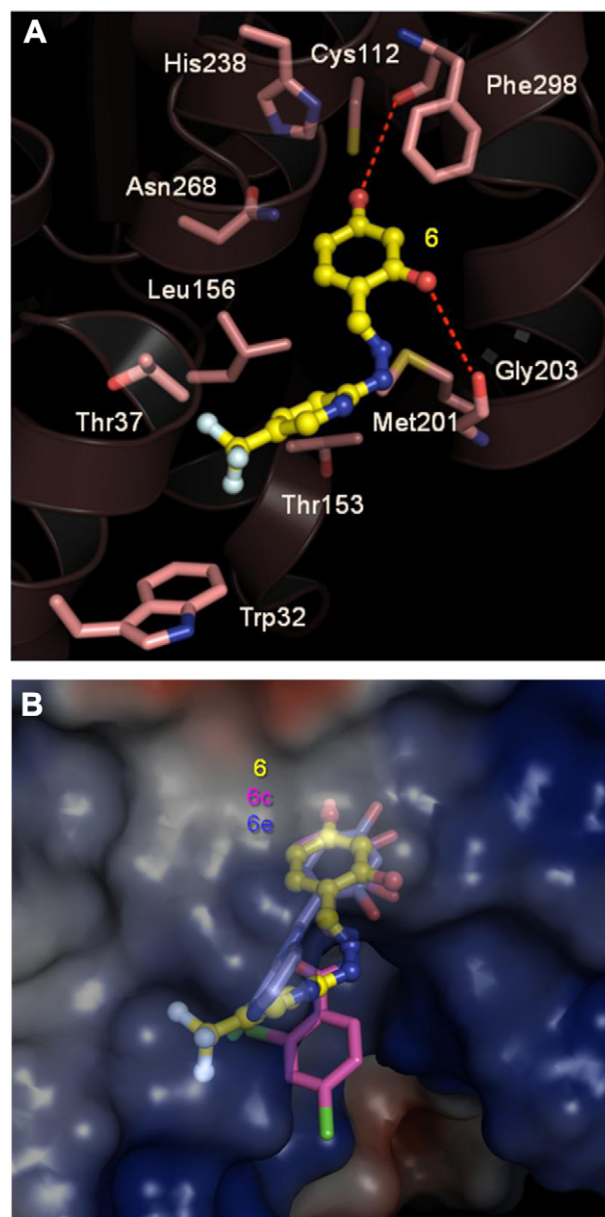


Fig. 5. Binding model of KAS III and three potent KAS III inhibitors (**6**, **6c**, and **6e**). (A) Detailed and superimposed binding model of **6** and saKAS III. (B) Overlapped binding model of three saKAS III inhibitors. **6** is shown in yellow, **6c** in magenta, and **6e** in blue. (For interpretation of the references to colour in this figure legend, the reader is referred to the web version of this article.)

YKAs3003 has a Schiff base moiety, whereas **6** has a hydrazone moiety. We hypothesize that the hydrazone group influences antimicrobial activity against the *S. aureus* bacterial strain, because the antimicrobial activity of **6** is much higher than that of YKAs3003 against *S. aureus* and MRSA. The hydrazone functionality has previously been shown to contribute to the biological activity of compounds, such as antimicrobial activity against several bacteria [44,45]. Several known antibiotics contain a hydrazone group, including rifampicin [46], which belongs to the rifamycin family, and cefazolin [47], a first generation cephalosporin class of antibiotic. Therefore, the hydrazone group in our compounds is likely a critical feature in the design of antimicrobial inhibitors of saKAS III.

It was necessary to identify the structural importance of the benzene-1,3-diol and hydrazone moieties (called 4-hydrazono-methyl-benzene-1,3-diol) to optimize our new KAS III inhibitors

with selectivity against *S. aureus* and MRSA. Therefore, we performed *in silico* screening to optimize the potency of **6** to find analogs with higher activities.

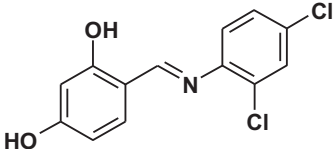
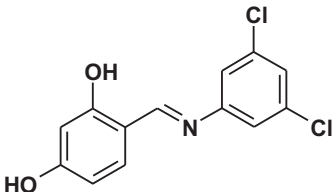
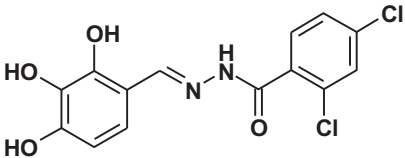
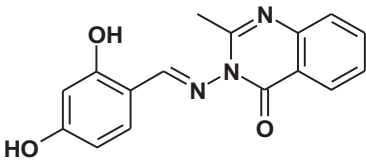
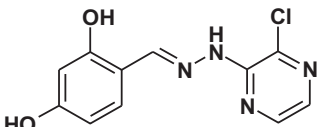
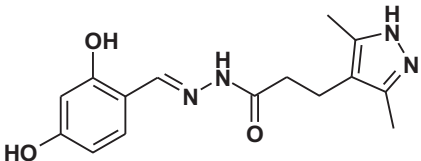
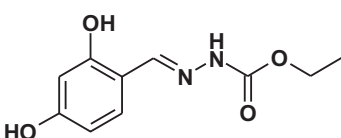
3.5. *In silico* screening for saKAS III inhibitors with **6** analogs

Each moiety of 4-iminomethyl-benzene-1,3-diol and 4-hydrazonomethyl-benzene-1,3-diol was taken as the template core structure in the search for analogs of **6**. In this screening, we

identified a new pharmacophore map (Map III) that included Map I and an additional hydrophobic feature (Lipo2) found in **6**. Lipo2 represents an additional hydrophobic interaction of the trifluoromethyl group of **6**. We thus performed *in silico* screening with these two pharmacophore maps (Map I and III).

We selected 430 analogs that included 4-iminomethyl-benzene-1,3-diol or 4-hydrazonomethyl-benzene-1,3-diol as a core structure from 750,000 synthetic compounds, and built an analog database. Among 430 analog compounds, 102 were hit by these two

Table 2
Structures, chemical properties (PSA and AlogP) and dissociation constants (K_d) of analogs of **6** as inhibitors of saKAS III.

Compound	Chemical structure	PSA	AlogP	K_d (μ M) saKAS III
6a		52.8	4.27	0.72
6b		52.8	4.27	0.61
6c		52.8	3.85	0.0072
6d		102.2	3.29	0.0009
6e		85.5	2.20	0.0003
6f		90.6	2.08	0.23
6g		110.6	1.56	1.48

maps. We selected seven analogs that were the highest ranked by LigScore and had a LogP value in the range of 2–3.5 and a PSA value in the range of 55–100 Å². The 2D structures of these seven compounds and their chemical scoring values are shown in Table 2.

3.6. Binding assay and antimicrobial activity of **6** analogs

We measured the K_d and antimicrobial activity of the seven analogs (**6a–6g**). All analogs and **6** exhibited high binding affinity to saKAS III. **6c**, **6d**, and **6e** had extremely high affinities, with K_d values as low as single-digit nanomolar. **6e** showed the highest binding affinity to saKAS III. The dissociation constants of the analogs are listed in Table 2.

All analogs except **6d** showed some antimicrobial activities against various bacteria (Table 3). Compound **6c** displayed broad-spectrum antimicrobial activity against all five bacterial strains in the range of 4–64 µg/mL, similar to that of **6**. **6e** showed very selective antimicrobial activity against only *S. aureus* and MRSA at an MIC of 1 µg/mL. **6**, **6c**, and **6e**, which had the highest binding affinities against saKAS III compared to the other two bacterial KAS III, showed excellent antimicrobial activities against *S. aureus* and MRSA. Therefore, high binding affinities resulted in strong antimicrobial activity, with specificity against *S. aureus* and MRSA. As such, these compounds may be potential candidates in the development of novel antibiotics against *S. aureus* and its resistant bacterial strains.

3.7. Binding models of **6** analogs and saKAS III

Compounds **6c** (2,4-dichloro-benzoic acid (2,3,4-trihydroxy-benzylidene)-hydrazide) and **6e** (4-[(3-chloro-pyrazin-2-yl)-hydrazonomethyl]-benzene-1,3-diol) were hit by Map I, implying that they have one hydrophobic interaction with saKAS III. Therefore, the additional hydrophobic interaction Lipo2 in Map III, which originated from the trifluoromethyl group of **6**, is not necessarily a critical feature for the design of saKAS III inhibitors.

As mentioned previously, the benzene-1,3 diol group of each compound participated in hydrogen bonding interactions with the backbone carbonyl oxygen atom of Gly203 and Phe298. Furthermore, the 1,3-dichloro-benzene ring of **6c** and 3-chloro-pyrazine of **6e** formed a hydrophobic interaction with Thr153, Leu156, and Met201 of saKAS III. The superimposed binding model of three potential inhibitors is depicted in Fig. 5B.

In this study, we confirmed that the compounds, including 4-hydrazonomethyl-benzene-1,3-diol structural moiety, are novel and potent antimicrobial inhibitors of saKAS III. Our further optimization will thus focus on decreasing compound cytotoxicity, while increasing their antimicrobial activity, and the analogs of our antibacterial compounds will be synthesized for the refinement of structure-activity relationship (SAR).

Table 3

Antimicrobial activities of analogues of **6** in various bacteria.

Compound	MIC (µg/mL)				
	<i>E. coli</i>	<i>E. faecalis</i>	VREF	<i>S. aureus</i>	MRSA
TLM	128	256	128	256	128
6	512	64	32	2	4
6a	64	>512	>512	128	128
6b	64	512	>512	64	128
6c	64	32	32	4	4
6d	>512	>512	>512	>512	> 512
6e	>512	>512	32	1	1
6f	256	>512	>512	128	128
6g	>512	>512	256	256	512

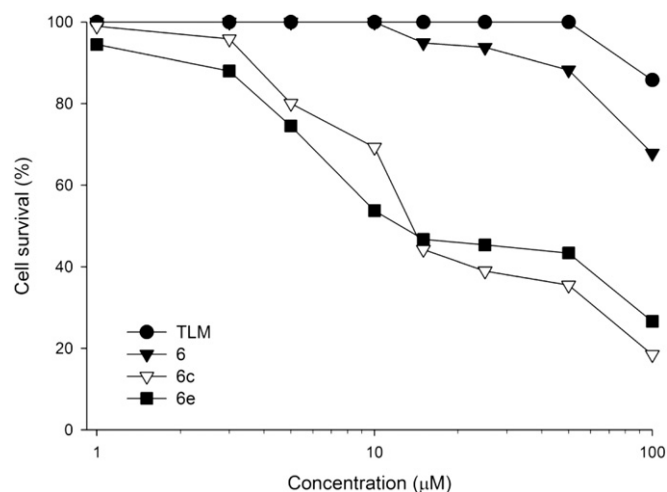


Fig. 6. Results of the MTT assay for the suggested KAS III inhibitors. This plot depicts the cell survival percentage values of NIH-3T3 versus the concentration of four antimicrobial inhibitors of KAS III.

3.8. Cytotoxicity of **6**, **6c**, and **6e**

The cytotoxicity of the three potent inhibitors against a mouse embryonic fibroblast cell line (NIH-3T3) was investigated using the MTT assay [48]. A plot of cell survival percentage values of NIH-3T3 cells versus the compound concentration is shown in Fig. 6. TLM and **6** showed over 85% and 67% cell survival at 100 µM, respectively. **6c** and **6e** showed lower IC₅₀ values (10.9 µM and 10.3 µM, respectively) against the normal fibroblast cells compared with TLM and **6**. However, at their MIC (1–4 µM), they were not cytotoxic to NIH-3T3 cells. It is possible that the antibacterial activities of **6c** and **6e** might be originated from cytotoxic effects. Therefore, the relationship between cytotoxicities and antimicrobial activities of these two compounds needs to be investigated and optimization needs to be done to reduce cytotoxicity in our further study.

4. Conclusion

In our two previous receptor-oriented pharmacophore-based *in silico* screenings of ecKAS III, we identified the lead compound YKAs3003 and confirmed the specificity of a pharmacophore map (Map I) to the design of antimicrobial KAS III inhibitors. Here, we determined two pharmacophore maps from receptor-oriented pharmacophore-based *in silico* screening of the x-ray structure of saKAS III to identify potent antimicrobial saKAS III inhibitors. We conducted biological assays and identified compound **6** as a novel and potent antimicrobial inhibitor of saKAS III. **6**, which has a 4-hydrazonomethyl-benzene-1,3-diol moiety, had a higher binding affinity, which increased its antimicrobial activity, compared to YKAs3003. The antimicrobial activity of **6** against *S. aureus* and MRSA was stronger than its activity against other bacteria, with an MIC value of 2–4 µg/mL. From these results, we confirmed the key role of the benzene-1,3-diol moiety on binding to saKAS III, which participates in hydrogen bonding interactions with side chains of the backbone oxygen of Phe304 and Gly209. We also verified the critical role of the hydrazone moiety on antimicrobial activity. In addition, we established the proper criteria of chemical scoring functions (AlogP and PSA) of KAS III inhibitors: AlogP values in the range of 2–3.5, and PSA values in the range of 55–100 Å².

To confirm the structural importance of the benzene-1,3-diol moiety and hydrazone moiety in **6**, we performed a fourth *in silico* screening with analog compounds of **6**. All nine selected analogs showed good binding affinity to all three bacterial KAS III enzymes

with micromolar to nanomolar dissociation constants. Eight analogs, except **6d**, showed good antimicrobial activity against various bacteria. **6c** and **6e**, which have the 4-hydrazonomethyl-benzene-1,3-diol structural moiety similar to **6**, showed an extremely high binding affinity for saKAS III and remarkable antimicrobial activities specifically against *S. aureus* and MRSA in the range of 1–4 µg/mL MIC. We can conclude that the 4-hydrazonomethyl-benzene-1,3-diol group is an essential functional moiety for the design of saKAS III inhibitors with powerful antimicrobial activity. This study shows that **6**, **6c**, and **6e** are novel compounds that can be potent antimicrobial inhibitors of saKAS III with selectivity against *S. aureus* and MRSA.

Acknowledgments

This work was supported by Basic Science Research Program through the National Research Foundation of Korea (NRF) funded by the Ministry of Education, Science and Technology (2009-0076064 and 2011-0022873) and by the Priority Research Centers Program through the National Research Foundation of Korea (NRF) funded by the Ministry of Education, Science and Technology (2009-0093824).

References

- [1] S. Stefani, A. Goglio, Methicillin-resistant *Staphylococcus aureus*: related infections and antibiotic resistance, *Int. J. Infect. Dis.* 4 (2010) S19–S22.
- [2] E. Tacconelli, G. De Angelis, M.A. Cataldo, E. Pozzi, R. Cauda, Does antibiotic exposure increase the risk of methicillin-resistant *Staphylococcus aureus* (MRSA) isolation? A systematic review and meta-analysis, *J. Antimicrob. Chemother.* 61 (2008) 26–38.
- [3] G.C. Schito, The importance of the development of antibiotic resistance in *Staphylococcus aureus*, *Clin. Microbiol. Infect.* 12 (2006) 3–8.
- [4] E. Turos, K.D. Revell, P. Ramaraju, D.A. Gergeres, K. Greenhalgh, A. Young, N. Sathyanarayan, S. Dickey, D. Lim, M.M. Alhamadsheh, K. Reynolds, Unsymmetric aryl-alkyl disulfide growth inhibitors of methicillin-resistant *Staphylococcus aureus* and *Bacillus anthracis*, *Bioorg. Med. Chem.* 16 (2008) 6501–6508.
- [5] H. Lu, P.J. Tonge, Inhibitors of FabI an enzyme drug target in the bacterial fatty acid biosynthesis pathway, *Acc. Chem. Res.* 41 (2008) 11–20.
- [6] R.J. Heath, S.W. White, C.O. Rock, Lipid biosynthesis as a target for antibacterial agents, *Prog. Lipid Res.* 40 (2001) 467–497.
- [7] J.Z. Lu, P.J. Lee, N.C. Waters, S.T. Prigge, Fatty acid synthesis as a target for antimalarial drug discovery, *Comb. Chem. High Throughput Screen.* 8 (2005) 15–26.
- [8] C.Y. Lai, J.E. Cronan, Beta-ketoacyl-acyl carrier protein synthase III (FabH) is essential for bacterial fatty acid synthesis, *J. Biol. Chem.* 19 (2003) 51494–51503.
- [9] R.J. Heath, C.O. Rock, Inhibition of beta-ketoacyl-acyl carrier protein synthase III (FabH) by acyl-acyl carrier protein in *Escherichia coli*, *J. Biol. Chem.* 3 (1996) 10996–11000.
- [10] E. Christensen, B.B. Kragelund, P. von Wettstein-Knowles, A. Henriksen, Structure of the human beta-ketoacyl [ACP] synthase from the mitochondrial type II fatty acid synthase, *Protein Sci.* 16 (2007) 261–272.
- [11] Y.M. Zhang, S.W. White, C.O. Rock, Inhibiting bacterial fatty acid synthesis, *J. Biol. Chem.* 281 (2006) 17541–17544.
- [12] C. Davies, R.J. Heath, S.W. White, C.O. Rock, The 1.8 Å crystal structure and active-site architecture of beta-ketoacyl-acyl carrier protein synthase III (FabH) from *Escherichia coli*, *Structure* 8 (2000) 185–195.
- [13] K.S. Gajiwala, S. Margosiak, J. Lu, J. Cortez, Y. Su, Z. Nie, K. Appelt, Crystal structures of bacterial FabH suggest a molecular basis for the substrate specificity of the enzyme, *FEBS Lett.* 583 (2009) 2939–2946.
- [14] X. Qiu, A.E. Choudhry, C.A. Janson, M. Grooms, R.A. Daines, J.T. Lonsdale, S.S. Khandekar, Crystal structure and substrate specificity of the beta-ketoacyl-acyl carrier protein synthase III (FabH) from *Staphylococcus aureus*, *Protein Sci.* 14 (2005) 2087–2094.
- [15] R.A. Daines, I. Pendrak, K. Sham, G.S. Van Aller, A.K. Konstantinidis, J.T. Lonsdale, C.A. Janson, X. Qiu, M. Brandt, S.S. Khandekar, C. Silverman, M.S. Head, First X-ray cocrystal structure of a bacterial FabH condensing enzyme and a small molecule inhibitor achieved using rational design and homology modeling, *J. Med. Chem.* 46 (2003) 5–8.
- [16] A.C. Price, K.H. Choi, R.J. Heath, Z. Li, S.W. White, C.O. Rock, Inhibition of beta-ketoacyl-acyl carrier protein synthases by thiolactomycin and cerulenin. Structure and mechanism, *J. Biol. Chem.* 276 (2001) 6551–6559.
- [17] P. Kim, Y.M. Zhang, G. Shenoy, Q.A. Nguyen, H.I. Boshoff, U.H. Manjunatha, M.B. Goodwin, J. Lonsdale, A.C. Price, D.J. Miller, K. Duncan, S.W. White, C.O. Rock, C.E. Barry 3rd, C.S. Dowd, Structure-activity relationships at the 5-position of thiolactomycin: an intact (5R)-isoprene unit is required for activity against the condensing enzymes from *Mycobacterium tuberculosis* and *Escherichia coli*, *J. Med. Chem.* 49 (2006) 159–171.
- [18] J.M. McFadden, S.M. Medghalchi, J.N. Thupari, M.L. Pinn, A. Vadlamudi, K.I. Miller, F.P. Kuhajda, C.A. Townsend, Application of a flexible synthesis of (5R)-thiolactomycin to develop new inhibitors of type I fatty acid synthase, *J. Med. Chem.* 48 (2005) 946–961.
- [19] Z. Nie, C. Perretta, J. Lu, Y. Su, S. Margosiak, K.S. Gajiwala, J. Cortez, V. Nikulin, K.M. Yager, K. Appelt, S. Chu, Structure-based design, synthesis, and study of potent inhibitors of beta-ketoacyl-acyl carrier protein synthase III as potential antimicrobial agents, *J. Med. Chem.* 48 (2005) 1596–1609.
- [20] M.M. Alhamadsheh, N.C. Waters, S. Sachdeva, P. Lee, K.A. Reynolds, Synthesis and biological evaluation of novel sulfonyl-naphthalene-1,4-diols as FabH inhibitors, *Bioorg. Med. Chem. Lett.* 18 (2008) 6402–6405.
- [21] D. Sinha, A.K. Tiwari, S. Singh, G. Shukla, P. Mishra, H. Chandra, A.K. Mishra, Synthesis, characterization and biological activity of Schiff base analogues of indole-3-carboxaldehyde, *Eur. J. Med. Chem.* 43 (2008) 160–165.
- [22] K. Cheng, Q.Z. Zheng, Y. Qian, L. Shi, J. Zhao, H.L. Zhu, Synthesis, antibacterial activities and molecular docking studies of peptide and Schiff bases as targeted antibiotics, *Bioorg. Med. Chem.* 17 (2009) 7861–7871.
- [23] L. Shi, R.Q. Fang, Z.W. Zhu, Y. Yang, K. Cheng, W.Q. Zhong, H.L. Zhu, Design and synthesis of potent inhibitors of beta-ketoacyl-acyl carrier protein synthase III (FabH) as potential antibacterial agents, *Eur. J. Med. Chem.* 45 (2010) 4358–4364.
- [24] A. Ashek, S.J. Cho, A combined approach of docking and 3D QSAR study of beta-ketoacyl-acyl carrier protein synthase III (FabH) inhibitors, *Bioorg. Med. Chem.* 14 (2006) 1474–1482.
- [25] A. Ashek, A.A. San Juan, S.J. Cho, HQSAR study of beta-ketoacyl-acyl carrier protein synthase III (FabH) inhibitors, *J. Enzym. Inhib. Med. Chem.* 22 (2007) 7–14.
- [26] S. Singh, L.K. Soni, M.K. Gupta, Y.S. Prabhakar, S.G. Kaskhedikar, QSAR studies on benzoylaminobenzoic acid derivatives as inhibitors of beta-ketoacyl-acyl carrier protein synthase III, *Eur. J. Med. Chem.* 43 (2008) 1071–1080.
- [27] J.Y. Lee, K.W. Jeong, J.U. Lee, D.I. Kang, Y. Kim, Novel *E. coli* beta-ketoacyl-acyl carrier protein synthase III inhibitors as targeted antibiotics, *Bioorg. Med. Chem.* 17 (2009) 1506–1513.
- [28] J.Y. Lee, K.W. Jeong, S. Shin, J.U. Lee, Y. Kim, Antimicrobial natural products as beta-ketoacyl-acyl carrier protein synthase III inhibitors, *Bioorg. Med. Chem.* 17 (2009) 5408–5413.
- [29] CATALYST, Version 4.10 Software. Accelrys Inc, San Diego, CA, 2000.
- [30] N.W. Murrall, E.K. Davies, Conformational freedom in 3-D databases. 1. Techniques, *J. Chem. Inf. Comput. Sci.* 30 (1990) 312–316.
- [31] P. Purushottamachar, A. Khandelwal, P. Chopra, N. Maheshwari, L.K. Gediya, T.S. Vasaitis, R.D. Bruno, O.O. Clement, V.C. Njar, First pharmacophore-based identification of androgen receptor down-regulating agents: discovery of potent anti-prostate cancer agents, *Bioorg. Med. Chem.* 15 (2007) 3413–3421.
- [32] K.W. Jeong, J.Y. Lee, D.I. Kang, J.U. Lee, S.Y. Shin, Y. Kim, Screening of flavonoids as candidate antibiotics against *Enterococcus faecalis*, *J. Nat. Prod.* 72 (2009) 719–724.
- [33] J.D. MacLowry, M.J. Jaqua, S.T. Selepak, Detailed methodology and implementation of a semiautomated serial dilution microtechnique for antimicrobial susceptibility testing, *Appl. Microbiol.* 20 (1970) 46–53.
- [34] S. Dixon, W. Brumfitt, J.M. Hamilton-Miller, In vitro activity of six antibiotics against multidrug-resistant staphylococci and other gram-positive cocci, *Eur. J. Clin. Microbiol.* 4 (1985) 19–23.
- [35] S.C. Park, M.H. Kim, M.A. Hossain, S.Y. Shin, Y. Kim, L. Stella, J.D. Wade, Y. Park, K.S. Hahn, Amphipathic alpha-helical peptide, HP (2–20), and its analogues derived from *Helicobacter pylori*: pore formation mechanism in various lipid compositions, *Biochim. Biophys. Acta* 1778 (2008) 229–241.
- [36] A. Rizzo, M. Zanetti, R. Gennaro, Cytotoxicity and apoptosis mediated by two peptides of innate immunity, *Cell. Immunol.* 189 (1998) 107–115.
- [37] H. Suttman, M. Retz, F. Paulsen, J. Harder, U. Zwerger, J. Kamradt, B. Wullich, G. Unteregger, M. Stöckle, J. Lehmann, Antimicrobial peptides of the Cecropin-family show potent antitumor activity against bladder cancer cells, *BMC Urol.* 8 (2008) 5.
- [38] X. Qiu, C.A. Janson, W.W. Smith, M. Head, J. Lonsdale, A.K. Konstantinidis, Refined structures of beta-ketoacyl-acyl carrier protein synthase III, *J. Mol. Biol.* 307 (2001) 341–356.
- [39] V. Aparna, G. Rambabu, S.K. Panigrahi, J.A. Sarma, G.R. Desiraju, Virtual screening of 4-anilinoquinazoline analogues as EGFR kinase inhibitors: importance of hydrogen bonds in the evaluation of poses and scoring functions, *J. Chem. Inf. Model.* 45 (2005) 725–738.
- [40] C.M. Venkatachalam, X. Jiang, T. Oldfield, M. Waldman, LigandFit: a novel method for the shape-directed rapid docking of ligands to protein active sites, *J. Mol. Graph. Model.* 21 (2003) 289–307.
- [41] B.F. Jensen, H.H.F. Refsgaard, R. Broc, P.B. Brockhoff, Classification of membrane permeability of drug candidates: a methodological investigation, *QSAR Comb. Sci.* 24 (2005) 449–457.
- [42] D.F. Veber, S.R. Johnson, H.Y. Cheng, B.R. Smith, K.W. Ward, K.D. Kopple, Molecular properties that influence the oral bioavailability of drug candidates, *J. Med. Chem.* 45 (2002) 2615–2623.
- [43] B. Mishra, A. Barik, K.I. Priyadarsini, H. Mohan, Fluorescence spectroscopic studies on binding of a flavonoid antioxidant quercetin to serum albumins, *J. Chem. Sci.* 117 (2005) 641–647.
- [44] S. Rollas, G.S. Küçükgüzel, Biological activities of hydrazone derivatives, *Molecules* 12 (2007) 1910–1939.
- [45] F.R. Pavan, P.I. da, S. Maia, S.R. Leite, V.M. Deflon, A.A. Batista, D.N. Sato, S.G. Franzblau, C.Q. Leite, Thiosemicarbazones semicarbazones dithiocarbazates

- and hydrazide/hydrazones: anti-*Mycobacterium tuberculosis* activity and cytotoxicity, *Eur. J. Med. Chem.* 45 (2010) 1898–1905.
- [46] P. Sensi, N. Maggi, S. Furesz, G. Maffii, Chemical modifications and biological properties of rifamycins, *Antimicrob. Agents Chemother.* (Bethesda) 6 (1966) 699–714.
- [47] R.C. Moellering Jr., M.N. Swartz, Drug therapy: the newer cephalosporins, *N. Engl. J. Med.* 294 (1976) 24–28.
- [48] G.J. Todaro, H. Green, Quantitative studies of the growth of mouse embryo cells in culture and their development into established lines, *J. Cell Biol.* 17 (1963) 299–313.